

## Harmonic Dynamics in Supercooled Liquids: The Case of Water

Francesco Sciortino and Piero Tartaglia

*Dipartimento di Fisica and Istituto Nazionale per la Fisica della Materia, Università di Roma La Sapienza,  
P.le Aldo Moro 2, I-00185, Roma, Italy*

(Received 10 January 1997)

We present an analysis of the molecular motion in supercooled liquid states, based on the topology of the configurational phase space and using the instantaneous normal mode technique. We aim at characterizing the harmonicity of the dynamics and evaluating its role in the short-time dynamics. For supercooled water, we find that modes with frequency higher than  $40 \text{ cm}^{-1}$  have a very strong harmonic character and control, in the low- $T$  regime, the fast process of exploration of phase space around the local minima. The fast decay of correlation functions for time shorter than 1 ps is attributed mainly to a dephasing (as opposed to a relaxation) process. [S0031-9007(97)02742-7]

PACS numbers: 61.20.Lc, 61.20.Ja, 63.50.+x, 64.70.Pf

Deep supercooled liquids present a clear separation between the microscopic and structural relaxation dynamics [1]. At very short times (ps scale) molecules move in an almost frozen energy landscape, exploring a finite region of phase space around a local minimum (basin). At longer times, the system visits different basins exploring larger and larger phase-space regions [2,3]. On cooling, the intrabasin motion becomes more and more separated in time from the slow interbasin motion. As a result, memory of the initial configuration is often lost in a two-step process [4,5]. The time dependence of any normalized correlation function  $\phi(t)$  is affected by the presence of these two time scales. At short times  $\phi(t)$  goes from one to a plateau value  $\phi_p$  (fast relaxation), while on a longer time scale  $\phi(t)$  decays from  $\phi_p$  to zero ( $\alpha$  relaxation). During the fast relaxation, the system explores the original basin, while during the  $\alpha$ -relaxation process, the system visits larger and larger regions of phase space, restoring ergodicity. The last process controls molecular diffusion.

The nature of the fast relaxation process is the main point of this Letter. Two extreme scenarios can be depicted to describe the dynamics in this regime, after the trivial very short-time ballistic motion. In the first scenario, the potential confining the molecules is strongly anharmonic and oscillatory motions are overdamped. The system performs a diffusional process in the basin in which it is trapped and  $\phi(t)$  decays to  $\phi_p$  following an exponential law [6,7]. In the second extreme scenario, the confining potential is highly harmonic and molecules perform oscillatory motion. Again, correlation functions decay (in a nonexponential way) to the plateau value, but this time the fast decay of  $\phi(t)$  reflects the dephasing of all superimposed independent oscillations controlling the dynamics of the system [8–11].

In real systems, it would be very valuable to assess to which extent the observed decay to the plateau is due to a relaxation (as opposed to a dephasing) process [12]. This Letter is an effort in this direction for the case of supercooled liquid water, using the instantaneous

normal mode (INM) technique [13] to calculate the local curvature of the potential along all independent directions in phase space and to estimate the degree of harmonicity along each of these directions [14]. INM are calculated diagonalizing numerically the Hessian matrix, from equilibrated configurations at finite  $T$  [15]. Because the  $T$  is finite, the system is not sitting in a local minimum of the phase space and the curvature along a few directions  $\mathbf{e}_\omega$  is negative, implying that along these directions the potential is anharmonic. The negative curvature directions may lead to basin change as well as to confined anharmonic oscillations [16,17]. For these negative directions, the frequency is imaginary.

Figure 1 shows the INM spectrum at two  $T$ , both for positive and imaginary  $\omega$ . Following the notation of Ref. [18] we display the imaginary  $\omega$  as  $-|\omega^2|^{1/2}$ , to remind us of, with the presence of the minus sign, the negative curvature of the potential. The spectrum of real  $\omega$  can be decomposed in two regions, above and below  $400 \text{ cm}^{-1}$ , which separate the mainly translational modes from the mainly rotational modes [19,20]. On cooling the system, translational and rotational modes become better resolved. The spectrum of imaginary  $\omega$  is also  $T$

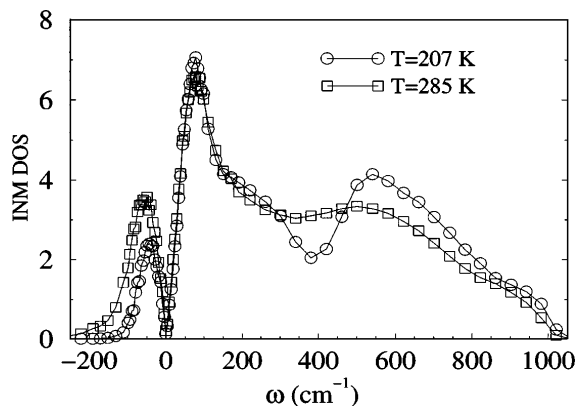


FIG. 1. Instantaneous density of states for SPC/E water at the lowest and highest studied temperatures.

dependent [21]. As stated above, negative eigenmodes correspond to two different types of curvature of the phase space. Some negative eigenmodes give rise to double well type of structures (*unstable modes*), i.e., can be associated with saddle points in phase space, while other negative eigenmodes arise from anharmonic terms in the potential energy (*shoulder modes*). An example of the profile of the potential energy along the direction  $\mathbf{e}_\omega$  for both types of negative eigenmodes is shown in Fig. 2. When the system moves along an unstable-mode direction, it may overcome the barrier and move to an adjacent distinct local minimum of the potential energy hypersurface. Motion along these directions is associated with global displacement (i.e., to diffusion) and to loss of coherence of the motion along direction with positive curvature of the potential [18,22]. Motion along all positive  $\omega$  and along shoulder eigenmodes describes the confined motion around one local minimum of the potential energy hypersurface.

The association of the unstable modes with diffusivity has been proposed and studied in some details in the last decade [18,21,23]. To corroborate the interpretation of diffusion as a result of the motion along the unstable directions, we show the  $T$  dependence of the fraction of negative, shoulder, and unstable modes in Fig. 3. Consistently with what is found in Ref. [17] for soft spheres, the fraction of unstable modes becomes very small close to the ideal kinetic glass transition  $T_c$  [24]. The fraction of shoulder modes decreases with  $T$  but remains finite at  $T_c$ . Thus, the switch of local minima becomes a rare event at low  $T$  and the system becomes confined in a finite region of phase space around a minimum.

To estimate the degree of harmonicity of positive curvature modes we calculate the potential energy along each  $\mathbf{e}_\omega$  and locate the local minimum. We then evaluate the curvature of the potential at the minimum  $\omega_{\min}^2$ .

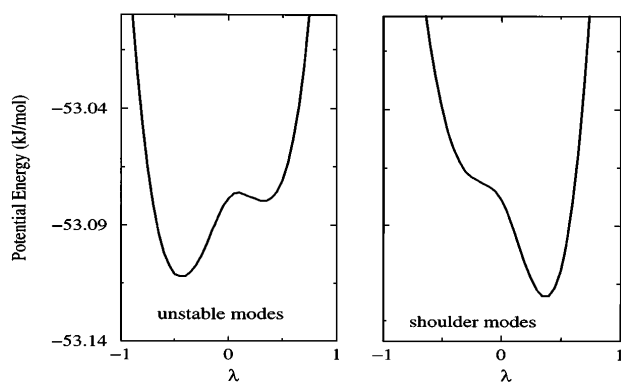


FIG. 2.  $V(\mathbf{X} + \lambda \mathbf{e}_\omega)$  for two selected eigenmodes  $\mathbf{e}_\omega$  at  $T = 207$  K.  $\mathbf{X}$  indicates the translational and rotational degrees of freedom. The left panel shows double-well unstable eigenmodes, while the right panel shows anharmonic shoulder eigenmodes.

For a truly harmonic potential, the ratio between the instantaneous curvature  $\omega_{\text{inst}}^2$  and  $\omega_{\text{min}}^2$  is one. The result is shown in Fig. 4. All rotational modes are essentially harmonic as well as all translational modes with  $\omega$  larger than about  $40 \text{ cm}^{-1}$  [25]. Lower  $\omega$  modes are instead progressively more and more anharmonic and act, together with the shoulder eigenmodes, as damping terms of the harmonic oscillating modes. Thus, we may view the dynamical evolution of all correlation functions as a collection of harmonic modes with frequency higher than  $40 \text{ cm}^{-1}$ , whose coherence is destroyed by the presence of a small fraction of shoulder (both positive and negative) modes, and on a longer time scale by basin hopping. For sufficiently short times, the harmonic modes will retain their coherence and any correlation function will decay to a plateau value (the  $\phi_p$  nonergodicity factor) simply due to the dephasing associated with the finite width of the density of states.

To estimate to which extent at low  $T$  the short-time dynamics is controlled by the harmonic dynamics, we compare the dynamical behavior of the fictitious harmonic system, obtained by exciting with  $k_B T$  all stable modes with  $\omega$  larger than  $10 \text{ cm}^{-1}$ , with the exact dynamics calculated solving the Newton equation for the same system. Figure 5 shows the self-density autocorrelation function  $\phi_s(t)$  as a function of time for the harmonic and the Newtonian systems. We note that  $\phi_s(t)$  decays to a  $q$ -dependent plateau value [the Lamb-Mössbauer factor (LMF)] after a few oscillations. In the case of Newtonian dynamics,  $\phi_s(t)$  relaxes to zero with the two-step process characteristic of supercooled liquids. The LMF, shown in the inset, is very similar for both systems. We note also that both  $\phi_s(t)$  show an oscillatory character at short times, due to the superposition of many independent modes. All independent undamped modes, weighted by the density of states, add coherently for short times and incoherently for large times, resulting in the

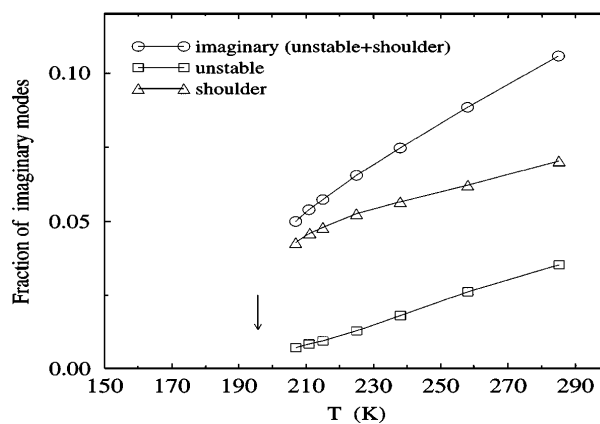


FIG. 3. Fraction of negative (circles), shoulder (triangles), and unstable (squares) eigenmodes as a function of  $T$ . The arrow locates  $T_c$ , the  $T$  at which the diffusivity extrapolate to zero (see Ref. [24]).

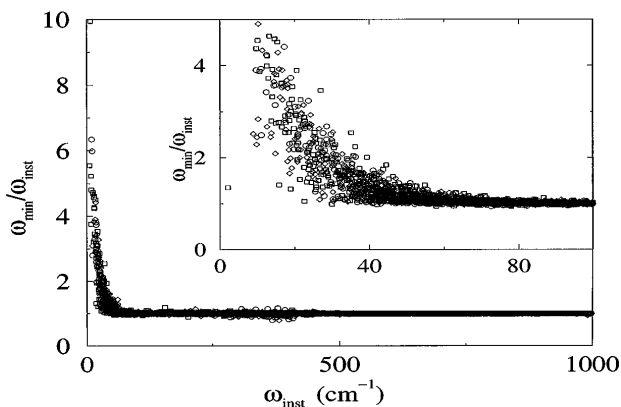


FIG. 4. Ratio of the instantaneous curvature ( $\omega_{\text{inst}}^2$ ) and the curvature at the associated minimum ( $\omega_{\text{min}}^2$ ) as a function of  $\omega_{\text{inst}}$  for  $T = 207, 238, 285$  K. Inset shows the low  $\omega$  part of the spectrum. Note that modes with  $\omega$  lower than  $40 \text{ cm}^{-1}$  are highly anharmonic. No  $T$  dependence is observed.

oscillatory behavior of  $\phi_s(t)$ . The different position of the oscillations between Newtonian and harmonic dynamics is related to both having neglected the confined anharmonic oscillations (which show up in the negative  $\omega$  region) and to the nonharmonicity of modes below  $40 \text{ cm}^{-1}$  which have been considered harmonic for computational purposes [26]. We note on passing that such oscillatory behavior in  $\phi_s(t)$  is also predicted in the Debye model for harmonic crystals [27].

The assumption that the harmonic dynamics is responsible for a large part of the delocalization of the system in phase space is not restricted to self-density. Figure 6 shows the  $q$ -vector dependence of the Debye-Waller fac-

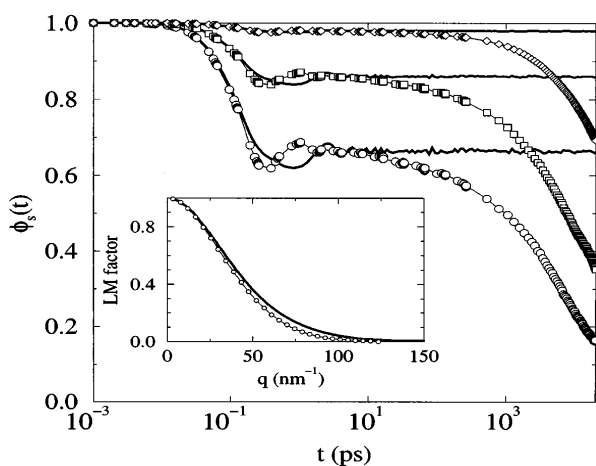


FIG. 5. Self-density autocorrelation function  $\phi_s(t)$  evaluated from the Newtonian dynamics (symbols) (from Ref. [24]) and from the harmonic dynamics (lines), both at  $T = 207$  K. Three different  $q$  vectors are shown.  $q = 6.6$  (diamonds),  $q = 18$  (squares), and  $q = 30$  (circles)  $\text{nm}^{-1}$ . Inset shows the  $q$  dependence of the plateau value (Lamb-Mössbauer factor) calculated as  $\phi_s(\infty)$  for the harmonic and as  $\phi_s(10 \text{ ps})$  for the Newtonian dynamics.

tor (DWF) for simulated water, i.e., the  $q$  dependence of the value of the density-density autocorrelation function after the fast dynamics. In the harmonic case, the DWF is defined as the long time limit of the density autocorrelation function in Fourier space and it gives information on the shape of the confining potential. In the Newtonian case, the DWF is estimated from the value of the density autocorrelation function at the plateau. The strong similarity between the two curves supports the view that the exploration of the basins in phase space is achieved significantly via harmonic dynamics.

In summary, we have presented an analysis of the INM in supercooled water, performed on the same configuration studied in Ref. [24] and previously analyzed in terms of mode coupling theory [5]. The vanishing in the number of directions leading to a different local basin in phase space appears to be the leading contribution to the vanishing of the diffusion constant. At the lowest temperature studied,  $T = 207$  K, the fraction of unstable modes is about 0.6%. At this low temperature, the motion of the system is confined in a finite part of its phase space for long time, and the harmonicity of the INM dictates how well response functions can be interpreted as a sum of harmonic motions. A measure of the remaining anharmonicity in the motion around  $T_c$  can be obtained by the fraction of shoulder modes at  $T_c$ . Water is characterized by a rather small number of imaginary modes compared, for example, to liquid argon [17], suggesting that motion over short-time scales can be approximated rather well with a harmonic dynamics. It is worth investigating in a future work the possibility that the fraction of imaginary modes correlates with the fragility of the liquid and with spectral signatures obeying boson statistics [1]. In the case of water, the strong harmonic character of molecular motion for  $\omega$  higher than  $40 \text{ cm}^{-1}$  suggests also a reconsideration of the high-frequency sound phenomena [28,29].

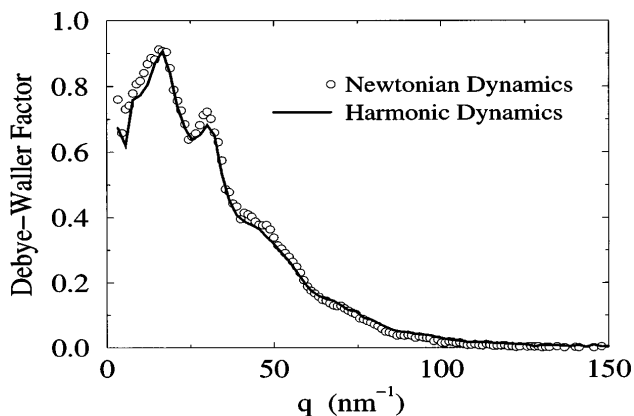


FIG. 6.  $q$  dependence of the plateau value for the density-density autocorrelation function  $\langle \rho_q(t) \rho_{-q}(0) \rangle$  (Debye-Waller factor) calculated as  $\langle \rho_q(\infty) \rho_{-q}(0) \rangle$  for the harmonic and as  $\langle \rho_q(10 \text{ ps}) \rho_{-q}(0) \rangle$  for the Newtonian dynamics, both at  $T = 20$  K.

The presence of a significant fraction of harmonic modes affects the behavior of the correlation functions at short times. The coherent motion of the harmonic oscillators leaves its imprinting in the correlation functions, which can be rather well described by the sum of the correlation function of each independent mode. This seems to suggest that, in water, the exploration of the phase space around the local minima in supercooled states is controlled by a dephasing, as opposed to a relaxation, process.

We thank C.A. Angell, W. Kob, and S. Sastry for useful discussions.

- 
- [1] C. A. Angell, *Science* **267**, 1924 (1995).  
 [2] F. H. Stillinger, *Science* **267**, 1935 (1995).  
 [3] M. Goldstein, *J. Chem. Phys.* **51**, 3728 (1969).  
 [4] For recent review see articles in *Science* **267** (1995), and M. D. Ediger, C. A. Angell, and S. R. Nagel, *J. Phys. Chem.* **100**, 13 200 (1996).  
 [5] W. Götze and L. Sjögren, *Rep. Prog. Phys.* **55**, 241 (1992).  
 [6] K. L. Ngai and K. Y. Tsang, *Macromol. Symp.* **90**, 95 (1995).  
 [7] J. Colmenero, A. Alegria, A. Arbe, and B. Frick, *Phys. Rev. Lett.* **69**, 478 (1992); J. Colmenero *et al.*, *Mater. Res. Soc. Symp. T Proc.* (to be published).  
 [8] U. Buchenau, C. Schönfeld, D. Richter, K. Kaji, T. Tanaka, and R. Wehrmann, *Phys. Rev. Lett.* **73**, 2344 (1994); U. Buchenau, *J. Non-Cryst. Solids* **172-174**, 391 (1994).  
 [9] A. P. Sokolov *et al.*, *Phys. Rev. Lett.* **71**, 2062 (1993); A. P. Sokolov, *Mater. Res. Soc. Symp. T Proc.* (to be published).  
 [10] For the sake of clarity, we do not discuss the distribution in the basin geometries which would require an additional average over their distribution. Such average may originate the self-similar dynamics predicted by mode coupling on approaching  $\phi_p$  [5].  
 [11] T. Keyes, *J. Chem. Phys.* **104**, 9349 (1996).  
 [12] The presence of a persistent harmonic dynamics could also explain the boson peak in the Raman spectrum [8,9].  
 [13] For a recent review on the INM technique see T. Keyes, *J. Phys. Chem.* (to be published). The first INM calculation goes back to A. Rahman, M. Mandell, and J. P. McTague, *J. Chem. Phys.* **64**, 1564 (1976). See also M. Buchner, B. M. Ladanyi, and R. M. Strat, *J. Chem. Phys.* **97**, 8522 (1992).  
 [14] INM analysis of liquid water at one state point under normal conditions has been presented in Ref. [19].  
 [15] We have analyzed the same configurations studied in Ref. [24], i.e., 50 equispaced independent configurations for each  $T$ , extracted from a molecular dynamics simulation based on the SPC/E potential. See Ref. [24] for details on the simulation.  
 [16] R. M. Cotterill and J. U. Madsen, *Phys. Rev. B* **33**, 262 (1985).  
 [17] S. D. Bembenek and B. B. Laird, *J. Chem. Phys.* **104**, 5199 (1996).  
 [18] G. Seeley, T. Keyes, and B. Madan, *J. Chem. Phys.* **95**, 3847 (1991); B. Madan, T. Keyes, and G. Seeley, *J. Chem. Phys.* **94**, 6762 (1991); **92**, 7565 (1990).  
 [19] M. Cho, G. R. Fleming, S. Saito, I. Ohmine, and R. Strat, *J. Chem. Phys.* **100**, 6672 (1994).  
 [20] In the translational region, we find the  $60\text{ cm}^{-1}$   $T$ -independent peak (oxygen-oxygen-oxygen bending) and an intense  $T$  dependent shoulder (oxygen-oxygen stretching) [28].  
 [21] U. Zürcher and T. Keyes (to be published); U. Zürcher, T. Keyes, and B. B. Laird (to be published).  
 [22] P. Moore and T. Keyes, *J. Chem. Phys.* **100**, 6709 (1994).  
 [23] J. E. Adams and R. M. Strat, *J. Chem. Phys.* **93**, 1632 (1990).  
 [24] F. Sciortino, P. Gallo, P. Tartaglia, and S. H. Chen, *Phys. Rev. E* **54**, 6331 (1996); *Phys. Rev. Lett.* **76**, 2730 (1996).  
 [25] We do not observe a significant  $T$  dependence in the nonharmonicity. Above  $40\text{ cm}^{-1}$  modes remain harmonic even when the  $T$  dependent amplitude of oscillation increases.  
 [26] Because the low  $\omega$  modes (which have the largest amplitudes and the longest coherence) are cut by the finite size of the simulated box, amplitude and position of the peak in  $\phi_s(t)$  may change on going to larger system sizes [J. Horbach, W. Kob, K. Binder, and C. A. Angell, *Phys. Rev. E* **54**, R5897 (1996)] although the feature is a genuine effect produced by the harmonic motion.  
 [27] G. H. Vineyard, *Phys. Rev. A* **110**, 999 (1958).  
 [28] F. Sciortino and S. Sastry, *J. Chem. Phys.* **100**, 3881 (1994).  
 [29] F. Sette, G. Ruocco, M. Krisch, U. Bergmann, C. Masciovecchio, V. Mazzacurati, G. Signorelli, and R. Verbeni, *Phys. Rev. Lett.* **75**, 152 (1995).